

## Supporting information

A systematic molecular simulation study of ionic liquid surfaces using intrinsic analysis methods

György Hantal<sup>1,2</sup>, Iuliia Voroshylova<sup>2</sup>, M. Natália D S Cordeiro<sup>2</sup> and Miguel Jorge<sup>1,\*</sup>

<sup>1</sup>LSRE – Laboratory of Separation and Reaction Engineering – Associate Laboratory LSRE/LCM, Faculdade de Engenharia, Universidade do Porto, Rua Dr. Roberto Frias, 4200-465 Porto, Portugal

<sup>2</sup>REQUIMTE – Associate Laboratory, Faculdade de Ciências, Universidade do Porto, Rua do Campo Alegre, 687, 4169-007 Porto, Portugal

Additional Figures obtained from the intrinsic analysis and orientation analysis of the ionic liquid interfaces.

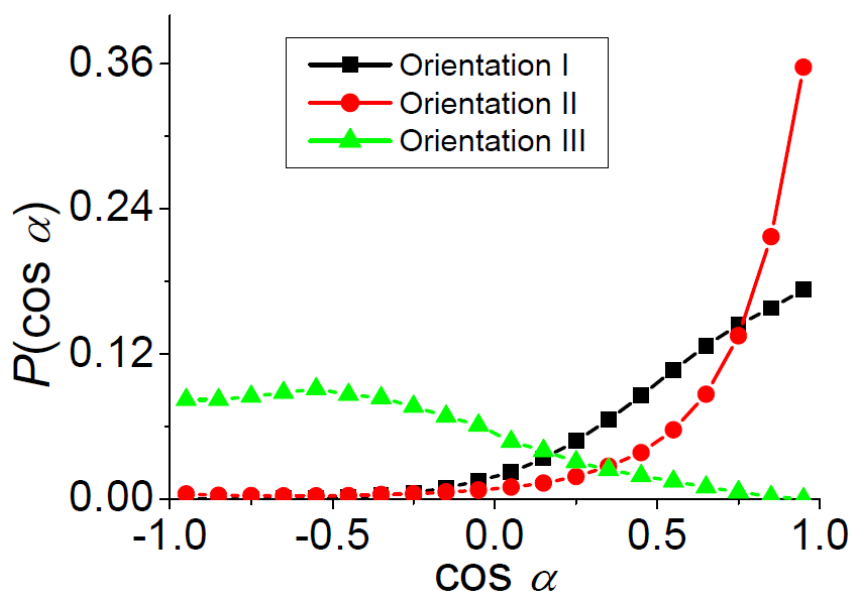


Figure S1 – Probabilities for the angle between the surface normal and the vector pointing from the first carbon atom of the butyl chain (C13) to the terminal one (C22). Each curve corresponds to a region dominated by one of the preferred ring orientations, as defined by the blue rectangles in Figure 6 of the paper.

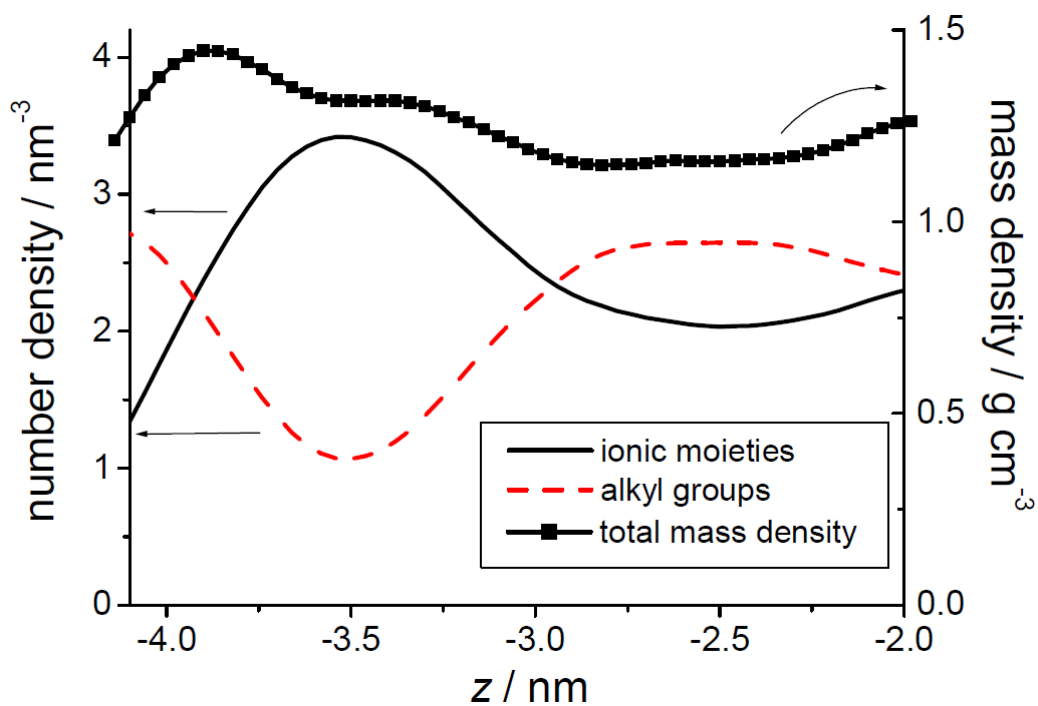


Figure S2 –Global number density profiles averaged over individual sites belonging to ionic moieties (black solid line) and alkyl groups (red dashed line). Global mass density profile for the whole system is also plotted (black squares with solid black line).The scale highlights the region of the density enhancement near the surface, dominated by ionic moieties, and the region of depleted density further into the liquid phase, dominated by alkyl groups.

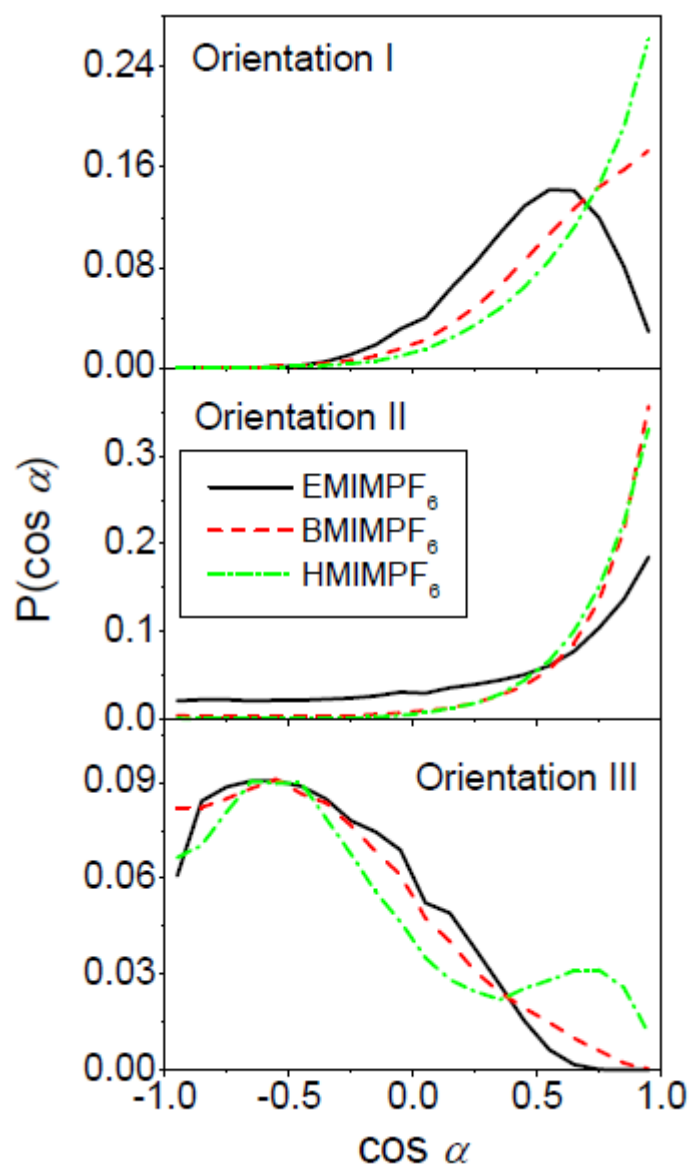


Figure S3 – Probabilities for the angle between the surface normal and the vector pointing from the first carbon atom of the butyl chain (C13) to the terminal one (C16, C22 and C28 for EMIM, BMIM and HMIM, respectively) in ILs with different cation alkyl chain length. The top panel is for rings in orientation I, the middle panel for orientation II and the lower panel for orientation III, as defined by the blue rectangles in Figure 6 of the paper.

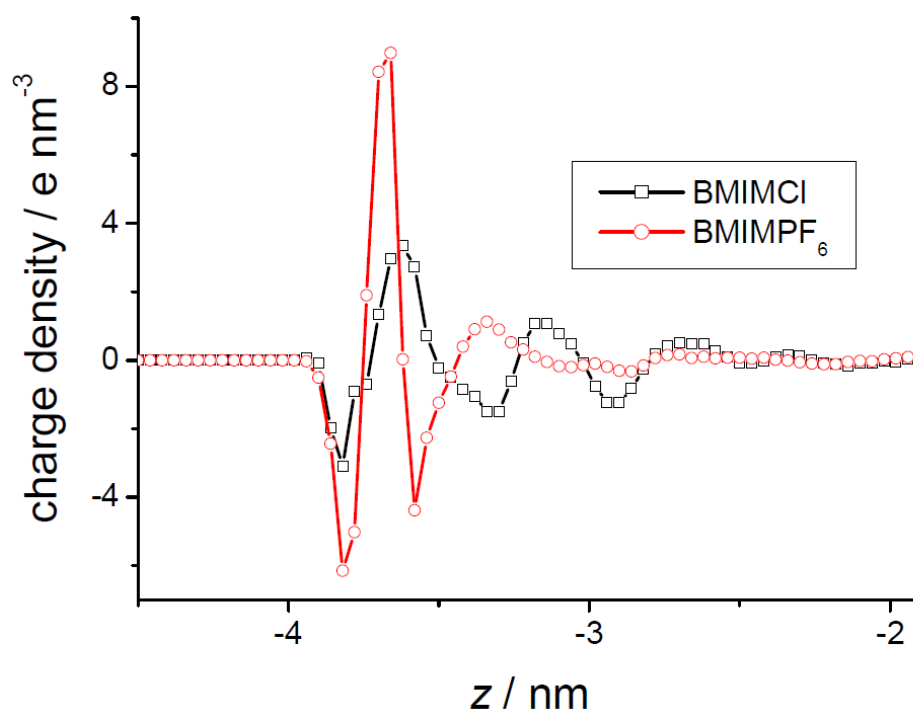


Figure S4 – Intrinsic electron density profiles across the interface of BMIMCl (open squares, black curve) and BMIMPF<sub>6</sub> (open circles, red curve) at 360 K.

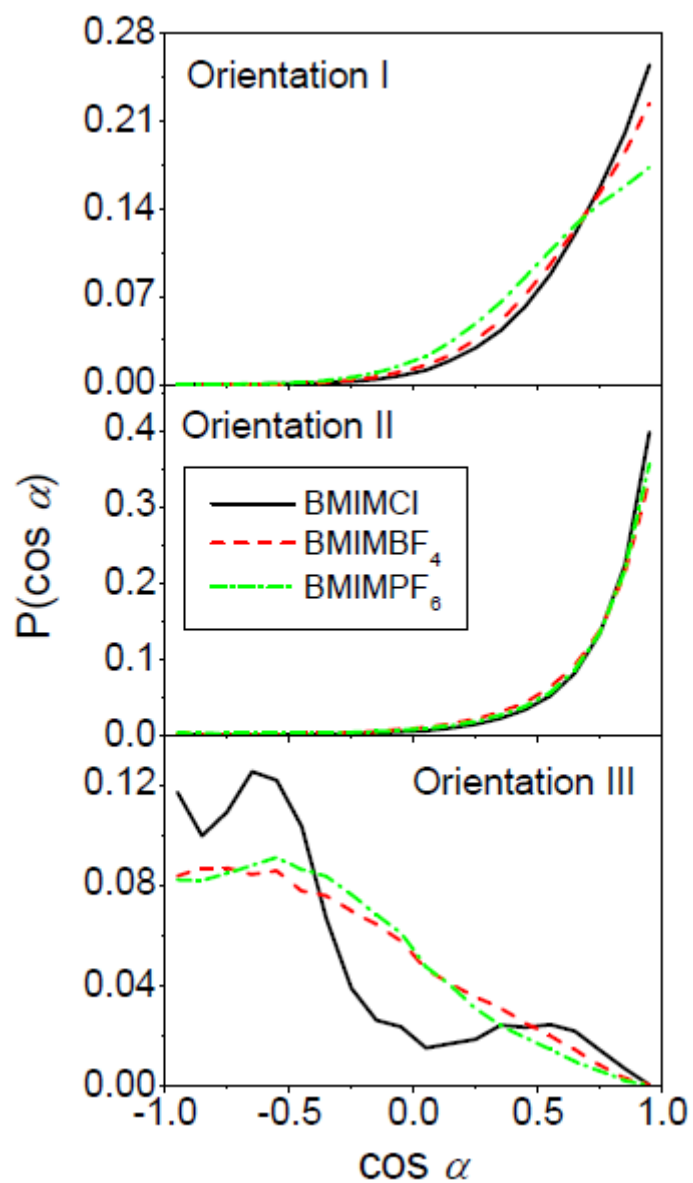


Figure S5 – Probabilities for the angle between the surface normal and the vector pointing from the first carbon atom of the butyl chain (C13) to the terminal one (C22) in ILs with different anions. The top panel is for rings in orientation I, the middle panel for orientation II and the lower panel for orientation III, as defined by the blue rectangles in Figure 6 of the paper.

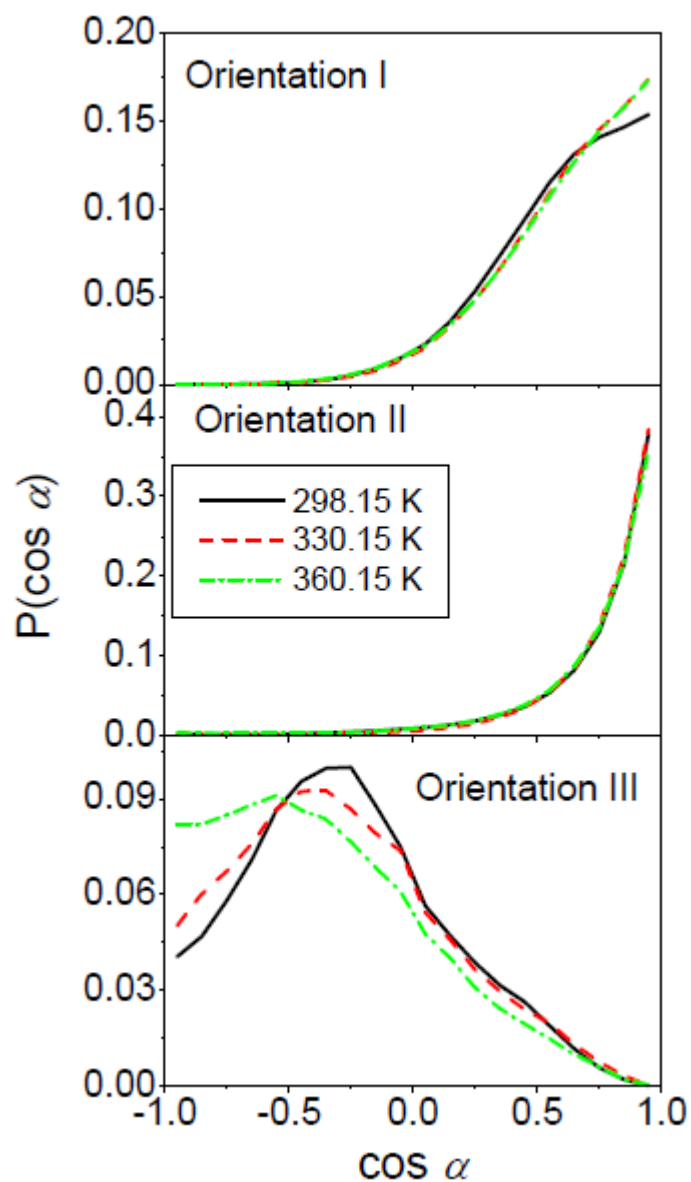


Figure S6 – Probabilities for the angle between the surface normal and the vector pointing from the first carbon atom of the butyl chain (C13) to the terminal one (C22) in BMIMPF<sub>6</sub> at different temperatures. The top panel is for rings in orientation I, the middle panel for orientation II and the lower panel for orientation III, as defined by the blue rectangles in Figure 6 of the paper.

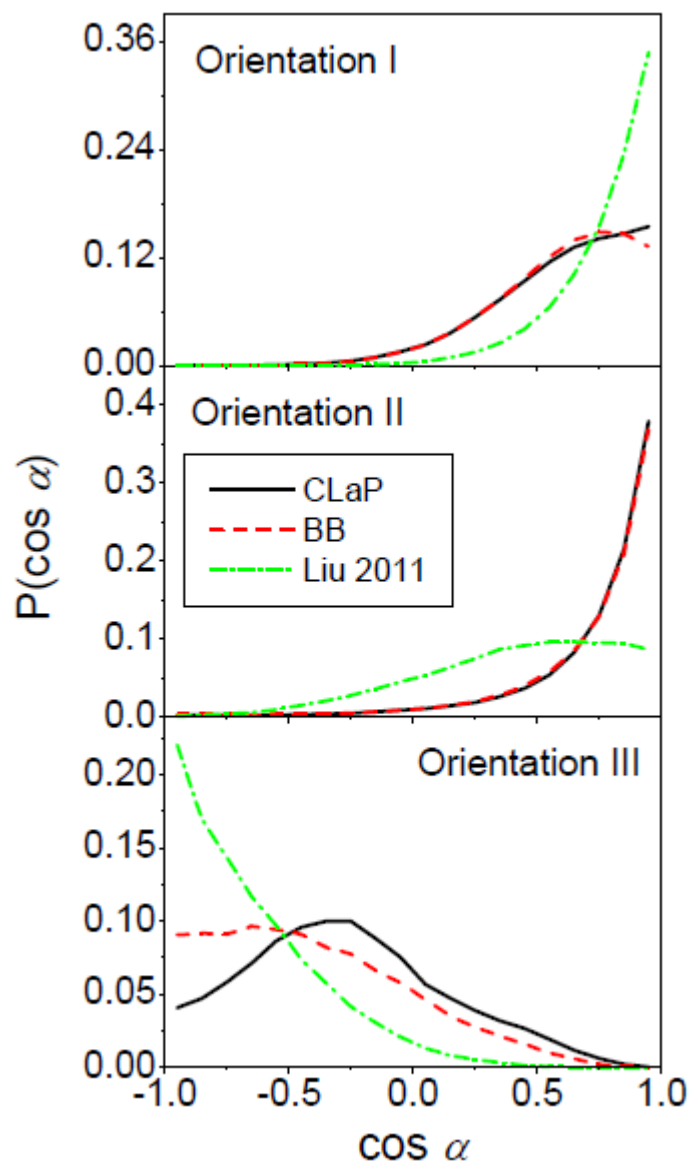


Figure S7 – Probabilities for the angle between the surface normal and the vector pointing from the first carbon atom of the butyl chain (C13) to the terminal one (C22) in BMIMPF<sub>6</sub> at 298 K using different molecular models. The top panel is for rings in orientation I, the middle panel for orientation II and the lower panel for orientation III, as defined by the blue rectangles in Figure 6 of the paper.